Embedded-atom-method study of structural, thermodynamic, and atomic-transport properties of liquid Ni-Al alloys

Mark Asta
Sandia National Laboratories, MS 9161, P.O. Box 969, Livermore, California 94551-0969

Dane Morgan*
University of California at Berkeley, Berkeley, Califonia 94720

J. J. Hoyt
Sandia National Laboratories, MS 9161, P.O. Box 969, Livermore, California 94551-0969

Babak Sadigh
Lawrence Livermore National Laboratories, Livermore, California 94550

J. D. Althoff and D. de Fontaine
University of California at Berkeley, Berkeley, Califonia 94720

S. M. Foiles
Sandia National Laboratories, MS 9161, P.O. Box 969, Livermore, California 94551-0969
(Received 9 December 1998)

Structural, thermodynamic, and atomic-transport properties of liquid Ni-Al alloys have been studied by Monte Carlo and molecular-dynamics simulations based upon three different embedded-atom method (EAM) interatomic potentials, namely those due to Foiles and Daw (FD) [J. Mater. Res. **2**, 5 (1987)], Voter and Chen (VC) [in *Characterization of Defects in Materials*, edited by R. W. Siegel *et al.* MRS Symposia Proceedings. No. 82 (Materials Research Society, Pittsburgh, 1987), p.175] and Ludwig and Gumbsch (LG) [Model. Simul. Mater. Sci. Eng. **3**, 533 (1995)]. We present detailed comparisons between calculated results and experimental data for structure factors, atomic volumes, enthalpies of mixing, activities, and viscosities. Calculated partial structure factors are found to be in semiquantitative agreement with published neutron scattering measurements for $Ni_{20}Al_{80}$ alloys, indicating that short-range order in the liquid phase is qualitatively well described. Calculated thermodynamic properties of mixing are found to agree very well with experimental data for Ni compositions greater than 75 atomic %, while for alloys richer in Al the magnitudes of the enthalpies and entropies of mixing are significantly underestimated. The VC and LG potentials give atomic densities and viscosities in good agreement with experiment for Ni-rich compositions, while FD potentials consistently underestimate both properties at all concentrations. The results of this study demonstrate that VC and LG potentials provide a realistic description of the thermodynamic and atomic transport properties for Ni_xAl_{1-x} liquid alloys with $x \geqslant 0.75$, and point to the limitations of EAM potentials for alloys richer in Al. [S0163-1829(99)02221-3]

I. INTRODUCTION

Structural, thermodynamic, and atomic-transport (viscosity, diffusion) properties of liquid Ni-Al alloys play important roles in the processing of commercial superalloys, and are therefore of significant practical interest. Ni-Al alloys are strongly ordering in the solid state and appreciable chemical short-range order (CSRO) is known to exist in the liquid phase as well.[1] Ni-Al is therefore interesting from a more basic point of view as a model system for studying CSRO and its consequences for physical properties in liquid-metal alloys.

A relatively large amount of experimental work has been devoted to the study of liquid Ni-Al. Maret *et al.*[1] used isotope substitution and neutron scattering to measure each of the three independent partial structure factors in a liquid $Ni_{20}Al_{80}$ alloy at $T=1300$ K. The Ni-Ni and Ni-Al partial structure factors showed a significant prepeak and preminimum, respectively, the origins of which can be attributed to an appreciable degree of CSRO in the liquid phase. Consistent with the presence of CSRO, measured enthalpies of mixing[2–5] in the liquid phase are large and negative, and chemical activities,[6–8] atomic volumes,[9] entropies,[10] and viscosities,[11] are characteristic of a highly nonideal solution.

The structural and thermodynamic properties of liquid Ni-Al alloys have been the topics of several theoretical studies.[12–16] Saadeddine *et al.*[15] analyzed the structure of liquid $Ni_{20}Al_{80}$ using a simple model based upon hard-sphere plus square-well interatomic potentials. These authors showed that a hard-sphere model gives an inadequate description of the liquid alloy structure, and it is necessary to model the attractive interactions between Ni and Al atoms in order to reproduce the CSRO features present in the measured structure factors. An additional study of the structure

of liquid $Ni_{20}Al_{80}$ was performed by Phuong, Manh, and Pasturel[14] using molecular-dynamics simulations based upon interatomic forces derived from a tight-binding-bond approach. These calculations produced partial structure factors in nearly perfect agreement with measurements, and demonstrated the importance of Al-Ni *p-d* electronic hybridization in governing the interatomic interactions between Ni and Al. Phuong *et al.* did not, however, report any results for thermodynamic or transport properties in Ni-Al. The most detailed theoretical studies of thermodynamic properties of liquid Ni-Al alloys were undertaken by Landa and co-workers[13] using pseudopotential, pertubation-theory approaches. Two different sets of calculations were performed using local and nonlocal pseudopotential formalisms, respectively. The nonlocal pseudopotential calculations, in which charge transfer was taken into account explicitly, produced results displaying the best overall agreement with experimental measurements. In particular, the experimentally observed, highly nonideal concentration dependence of the enthalpy, volume, entropy, and viscosity were reproduced in these calculations, although calculated values for the enthalpies of mixing were found to be larger in magnitude than measurements by as much as a factor of three (1.5 eV/atom).

Despite the fact that much theoretical work has been devoted to the properties of liquid Ni-Al alloys, it remains of interest to perform a systematic computational study of the structural, thermodynamic *and* transport properties within a single theoretical framework. In this paper the results of such a study, using computer simulations based upon the embedded-atom method (EAM),[17] are presented. The goal of this work is to study the relationship between liquid structure and thermodynamic and kinetic properties, as well as to use the extensive amount of experimental and theoretical data available for liquid Ni-Al as a means of critically testing the accuracy of the EAM in its application to the study of liquid transition-metal-Al alloys.

The EAM is a semiempirical, interatomic-potential method which has been applied widely in the study of crystalline metals and alloys.[18] The first EAM study of *liquids* was performed by Foiles[19] who found excellent agreement between EAM-simulated and experimentally measured[20] structure factors of elemental metals. Since this original work, the EAM has been used extensively to study the structural, thermodynamic, and dynamic properties of elemental liquids and glasses; the most successful applications have been for late transition, noble, and ''simple'' (*s-p*) metals.[21–44] Less work has been performed applying the EAM to the study of liquid and amorphous *alloys*.[45–50]

In EAM studies of liquids, it is important to consider that interatomic potentials are derived most readily by fitting to properties of crystalline phases. It is therefore a matter of practical interest to critically test the accuracy of results calculated for liquids using potentials derived solely from solid-state properties. The results mentioned above seem to indicate that for many properties of *elemental* liquid metals such potentials are adequate. Whether this is also the case for liquid *alloys* remains unclear. Ni-Al represents an ideal alloy system for testing the accuracy of EAM potentials for two reasons. First, as discussed above, there exists an extensive database of experimental measurements and calculated results for this system. Secondly, several EAM potentials have been developed for Ni-Al (for a review see Baskes[51]) using different functional forms for the pair potential terms, and fitting to different sets of elemental and alloy properties. The effects of such details upon calculated liquid-alloy properties are explored in this work by performing calculations using a total of three different Ni-Al potentials.[52–54]

The remainder of this paper is organized as follows: in the next section the details of the simulations and EAM potentials used in this study are described. A discussion of the liquid structure is given in Sec. III A where results for $Ni_{20}Al_{80}$ alloys are compared with the neutron-scattering measurements of Maret *et al.*[1] Calculated thermodynamic and transport properties are compared with available experimental data in Sec. III B and III C, respectively. Finally, the results are summarized.

II. METHOD

A. Interatomic potentials

Structural, thermodynamic and atomic-transport properties of liquid Ni-Al alloys have been computed using Monte Carlo (MC) and molecular dynamics (MD) simulations (see e.g., Ref. 55) based upon EAM energetics and interatomic forces. In this study calculations have been performed using three different Ni-Al potentials due to Voter and Chen (VC),[52] Foiles and Daw (FD),[53] and Ludwig and Gumbsch (LG).[54] The FD potentials were fit to the following set of experimental data: elastic constants, vacancy formation energies and cohesive energies for elemental Ni and Al, as well as cohesive energies and lattice constants for the alloy compounds Ni_3Al and NiAl. The VC potentials were fit to a slightly larger set of experimental data including (in addition to the properties used by FD): the bond-length and bond energy of the Ni-Ni and Al-Al diatomic molecules, as well as the elastic constants, vacancy formation energy, {100} and {111} antiphase boundary energies, and the superintrinsic stacking fault energy of Ni_3Al. A fundamental difference between the FD and VC potentials is associated with the detailed forms used for the pair interaction term. Specifically, in the FD parametrization[56] this term is purely repulsive, while the VC potential includes a medium-range attractive component.[52] In addition, the FD parametrization assumes that the Ni-Al pair potential is the harmonic mean of the Ni-Ni and Al-Al pair potentials, whereas the VC parametrization has independent fitting terms for the unlike pair interaction. We have performed calculations with both sets of potentials in order to study the effects upon simulated liquid-alloy properties associated with the detailed differences outlined in this paragraph.

Calculations also have been performed using the EAM potential due to Ludwig and Gumbsch (LG).[54] The LG potential makes use of functional forms very similar to VC, but more alloy properties are included in the fitting database. Specifically, Ludwig and Gumbsch include information about point defects in the NiAl compound, as well as first-principles-calculated energy barriers for shearing the NiAl lattice.[57] The LG calculations were performed in order to check whether predicted properties for liquid alloys are improved by the additional alloy information included in the fitting of the potentials.

B. Monte Carlo simulations

Structural and thermodynamic properties were computed using isothermal-isobaric MC simulations. Zero-pressure and periodic boundary conditions were used throughout, and simulations were performed in both canonical (C) (fixed number of Ni and Al atoms) and transmutation (TM) (fixed *total* number of atoms, variable number of Ni and Al atoms, fixed chemical potential *difference*) ensembles. In both types of simulations displacive degrees of freedom were sampled by attempting small atomic displacements (less than or equal to 0.1 Å) and changes in volume (the maximum allowed change in volume is 1%). Configurational degrees of freedom were sampled either by attempting a swap of two different atoms chosen at random (C), or by attempting a switch in an atom's type (TM).

Structure factors were computed by MC simulation as follows: after equilibrating a 2048-atom simulation (typically using 10^5 steps/atom in a C ensemble) periodic images of the final atomic configuration were used to generate a starting point for larger 16 384-atom simulations. In these larger simulations the structure was equilibrated over a few times 10^4 MC steps/atom, and subsequently 40 configurations were stored during a simulation involving an additional 20 000 MC steps/atom. These 40 configurations were analyzed in order to compute the total and partial (Ni-Ni, Ni-Al, and Al-Al) pair-correlation functions in real space, the Fourier transforms of which give the desired total and partial structure factors. The use of 16 384-atom simulations allowed us to ensure that small-q values for the structure factors were not appreciably affected by the use of a finite-sized simulation cell.

The concentration and temperature dependences of enthalpies, entropies, and free energies of mixing, as well as activites and atomic volumes, were computed by TM MC simulations. Specifically, at a given temperature 500-atom TM simulations were performed as a function of the imposed chemical field $(\Delta\mu=(\mu_{\mathrm{Ni}}-\mu_{\mathrm{Al}})/2)$ using 10^5 step/atom simulations (longer simulation times and the use of 2048-atom instead of 500-atom simulations were found to have very little effect upon the calculated results presented below). Enthalpies of mixing and atomic volumes were obtained directly from ensemble averages of the energy and volume evaluated during the simulations (the initial 10^4 steps/atom were not included in the averaging but were used for equilibration). These properties also can be readily computed from MD simulations. For alloys, however, MC simulations allow the chemical degrees of freedom to be sampled more efficiently.

Free energies, activities, and entropies of mixing were computed from TM EAM-MC calculations by thermodynamic integration based upon the relationship between the imposed values of $\Delta\mu$ and the average concentrations of Ni atoms (c) obtained from the simulations. Specifically, by integrating the following thermodynamic relation (where N is the total number of atoms, P is the pressure, T is the temperature, and ΔN is the difference between the number of Ni atoms N_{Ni} and the number of Al atoms N_{Al}):

$$\Delta\mu=\left(\frac{\partial G(N_{\mathrm{Al}},N_{\mathrm{Ni}},T,P)}{\partial\Delta N}\right)_{N,T,P} \tag{1}$$

the Gibbs free energy (G) difference between two alloys with compositions c_1 and c_2 can be obtained, giving

$$G(c_1,T,P,N)-G(c_2,T,P,N)=\int_{c_1}^{c_2}\Delta\mu(c,T,P)dc. \tag{2}$$

Equation (2) can be used to obtain Gibbs free energies of mixing provided the relationship $\Delta\mu(c,T,P)$ between the chemical field and composition is known for a given temperature and pressure. This relationship is easily obtained from the TM MC simulations described above. Once average values of c have been obtained via MC for a number of different values of the imposed chemical field, the following functional form is used to fit the data:

$$\Delta\mu(c,T,P)=\sum_{i=0}^{m} b_i(T,P)c^i+\frac{1}{2}k_BT\ln\frac{c}{1-c}. \tag{3}$$

In the above equation the last term on the right-hand side corresponds to an ideal solution, and the coefficients $[b_i(T,P)]$ in the polynomial expansion of the nonideal term (first term on right-hand side) are fit to MC data. It was found that roughly 20 data points and a third-order polynomial [i.e., $m=3$ in Eq. (3)] were sufficient to obtain well-converged free energies of mixing in this study. Once values of the mixing free energy have been computed, the entropy of mixing can be obtained by subtracting values of the enthalpies. Additionally, activities are readily computed from the free energy of mixing by differentiating the analytical expressions resulting from Eqs. (2) and (3).

C. Molecular-dynamics simulations

Three important atomic transport properties of liquid alloys which can be computed readily with molecular-dynamics simulations are: the shear viscosity, the chemical diffusivities and the mutual diffusion coefficient. The viscosity, η, is given by[58]

$$\eta=\frac{1}{k_BTV}\int_0^\infty\langle\sigma^{xz}(t)\sigma^{xz}(0)\rangle dt. \tag{4}$$

Here σ^{xz} is an off diagonal element of the stress tensor and the symbol $\langle\,\rangle$ denotes an average over all time origins (additional statistics were obtained by averaging over the equivalent yz and xy components of the stress tensor). The diffusivities of Ni and Al are obtained from an integral over the velocity-velocity correlation functions as[58]

$$D_i=\frac{1}{3}\int_0^\infty\langle\vec{u}_i(t)\cdot\vec{u}_i(0)\rangle dt \tag{5}$$

with $\vec{u}_i$ the velocity of atom type i. In the above expression the average is now performed over all time origins and over all atoms (of type i) in the system. (An alternative method for determining the diffusivities is through the limiting behavior of the mean-square displacement of the Ni or Al atoms.[58] It was found in the molecular-dynamics simulations that both techniques gave the same result to very high accuracy.) Finally, it is useful to examine the mutual diffusion coefficient, D_{NiAl}, which is defined by[58]

$$D_{\mathrm{NiAl}}=\frac{1}{3Nc_{\mathrm{Ni}}c_{\mathrm{Al}}}\int_0^\infty \langle \vec{J}^D(t)\cdot\vec{J}^D(0)\rangle dt. \tag{6}$$

Here $\vec{J}^D$ is the interdiffusion flux given by

$$\vec{J}^D(t)=c_{\mathrm{Ni}}\sum_{i\in \mathrm{Al}}\vec{u}_i(t)-c_{\mathrm{Al}}\sum_{j\in \mathrm{Ni}}\vec{u}_j(t), \tag{7}$$

where the summations over i and j are over all Al and Ni atoms, respectively. The molecular-dynamics algorithm employed in the present work has been utilized in numerous EAM studies of liquid and solid alloys [see, e.g., Ref. 18]. In all of the MD simulations starting configurations were obtained from the equilibrated 2048 atom structures of the Monte Carlo runs described above and initial atomic velocities were assigned randomly based on a Boltzmann distribution corresponding to the equilibrated temperature. After a brief equilibration time (10 ps), microcanonical (constant energy-volume-number) MD simulations were performed for a total of 40 ps using a time step of 1 fs. Even though the three correlation functions appearing in Eqs. (4)–(6) decayed to zero after a relatively short time ($\leqslant$0.5 ps) the long run times were necessary to achieve adequate statistics. Results for η, D_{Ni}, D_{Al}, and D_{NiAl} as a function of composition at 1900 K are presented in the next section.

III. RESULTS AND DISCUSSION

In this section we present results for liquid structure, thermodynamic properties of mixing, viscosities, and diffusion constants. These results are compared with available experimental data, as well as previous theoretical studies.

A. Liquid structure

The structure of liquid $Ni_{20}Al_{80}$ was investigated experimentally by Maret *et al.*[1] who used isotope substitution and neutron scattering to measure each of the three independent partial structure factors. The measured structure factors are reproduced with open symbols in Fig. 1, where results of FD and VC EAM-MC simulations are also shown (results obtained with LG potentials were found to be similar and are not included). In Figs. 1(a) and 1(b) results for Faber-Ziman[59] (FZ) and Bhatia-Thornton[60] (BT) structure factors are given. The FZ structure factors are defined as follows:

$$I_{ij}(\mathbf{q})=1+n\int d^3\mathbf{R}e^{i\mathbf{qR}}[g_{ij}(\mathbf{R})-1], \tag{8}$$

where n is the number density and g_{ij} is the usual partial pair-correlation function corresponding to species i and j. In terms of the FZ structure factors, the number-number (NN), chemical-chemical (CC), and number-chemical (NC) BT correlation functions are defined as follows:

$$S_{\mathrm{NN}}(\mathbf{q})=\sum_{ij} c_ic_jI_{ij}(\mathbf{q}), \tag{9a}$$

$$S_{\mathrm{CC}}(\mathbf{q})=c_Ac_B\{1+c_Ac_B[I_{AA}(\mathbf{q})+I_{BB}(\mathbf{q})-2I_{AB}(\mathbf{q})]\}, \tag{9b}$$

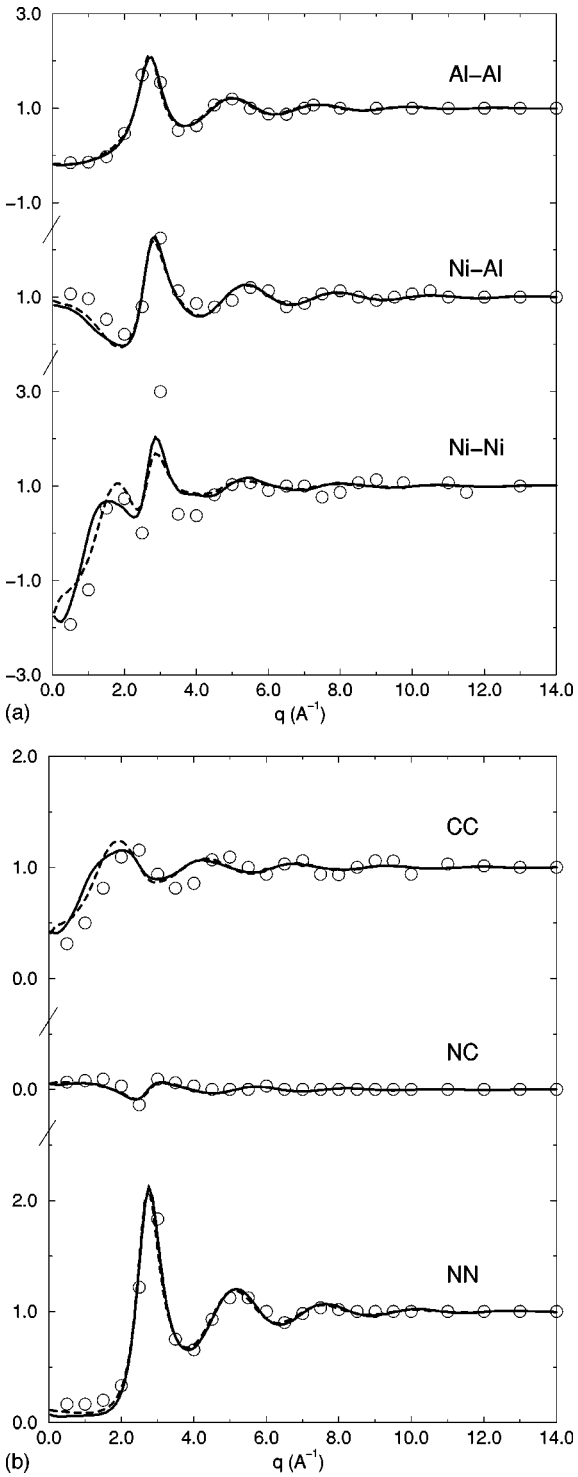

FIG. 1. Calculated and measured (a) Faber-Ziman and (b) Bhatia-Thornton partial structure factors for liquid $Ni_{20}Al_{80}$ at $T=1300$ K. Solid and dashed lines are calculated results obtained with Voter-Chen and Foiles-Daw EAM potentials, respectively. Open circles are taken from the measurements of Maret *et al.* (Ref. 1).

$$S_{\mathrm{NC}}(\mathbf{q})=c_Ac_B\{c_A[I_{AA}(\mathbf{q})-I_{AB}(\mathbf{q})]-c_B[I_{BB}(\mathbf{q})-I_{AB}(\mathbf{q})]\}, \tag{9c}$$

where c_A and c_B are concentrations of A and B atoms, respectively.

The measured FZ correlation functions reproduced in Fig. 1(a) display a significant prepeak and preminimum in the minority-minority (Ni-Ni) and heteroatomic (Ni-Al) partial structure factors, respectively, indicative of CSRO effects in the liquid.[1] In particular, as discussed further below, there is a tendency for Ni atoms to be surrounded by Al in the first-neighbor shell. The fact that the prepeak and preminimum in the structure factors shown in Fig. 1(a) originate from CSRO can be seen clearly from the BT correlation functions plotted in Fig. 1(b). S_{CC} shows a peak in the same position as the preminimum and prepeak in I_{NiAl} and I_{NiNi}, while no peaks in this position are seen in S_{NN}.

The solid and dashed lines in Figs. 1(a) and 1(b) correspond to EAM-MC results obtained with VC and FD potentials, respectively. Results obtained with FD, VC, and LG (not shown) potentials are found to be very similar, indicating that many of the structural features of the liquid are insensitive to the differences in the potentials mentioned in the previous section. In Fig. 1(a) it can be seen that the calculations reproduce the main features of the measured structure factors including the prepeak and preminimum in I_{NiNi} and I_{NiAl}, respectively. Furthermore, we find excellent quantitative agreement with measurements for the positions, heights, and widths of the peaks in I_{AlAl}, S_{NN}, and S_{NC}. The most significant discrepancies between calculations and measurements are found for I_{NiNi}, where EAM-MC results underestimate the depth and height of the first minimum and second peak, respectively.

The origin of CSRO in liquid Ni-Al alloys can be attributed to the strong interatomic interactions between Ni and Al, as discussed in detail by Saadeddine *et al.*[15] and Phuong *et al.*[14] More specifically, the CSRO is affected by the strength of the Ni-Al interaction relative to pure Ni-Ni and Al-Al interactions. The level of agreement between measurements and calculated structure factors shown in Fig. 1, suggests that the EAM describes reasonably well the relative strengths of the Ni-Ni, Ni-Al, and Al-Al interactions. The level of agreement shown in Fig. 1(b) is, however, not as good as that obtained by Phuong *et al.*, who made use of tight-binding theory to calculate interatomic interactions for Ni-Al. The tight-binding approach therefore appears to give rise to improved accuracy over EAM.

The local atomic structure of $Ni_{20}Al_{80}$ was discussed by Maret *et al.* based upon an analysis of partial pair-correlation functions, $G_{ij}(R)$, in real space. Maret *et al.* define $G_{ij}(R)$ as the Fourier transform of $q[I_{ij}(q)-1]$ and the same convention is followed here. Defined in this manner, the G_{ij} are simply related to the g_{ij} given in Eq. (8) by

$$G_{ij}(R)=4\pi Rn[g_{ij}(R)-1]. \tag{10}$$

In Fig. 2 we plot EAM results for G_{NiNi}, G_{NiAl}, and G_{AlAl}, obtained with VC and FD potentials for liquid $Ni_{20}Al_{80}$ at T=1300 K. As was the case for the calculated structure factors shown in Fig. 1, the two different sets of EAM results are found to be in excellent agreement. A significant difference between our results and those obtained by Maret *et al.* (see Fig. 7 of Ref. 1) is found for G_{NiNi}. In particular, Maret *et al.* find that the first peak in G_{NiNi} is split into two components centered at 2.36 and 2.98 Å , while we find only one peak centered at roughly 2.5 Å . While it is possible that this discrepancy may reflect the differences between the EAM-calculated and measured Ni-Ni structure factors shown in Fig. 1, it is interesting to consider that Phuong *et al.*[14] also find no indication of a split first peak for G_{NiNi} in their tight-binding-based MD calculations, even though their calculated structure factors are in nearly perfect agreement with measurements. In particular, Phuong *et al.* find a single first peak for G_{NiNi} centered around 2.55 Å in good agreement with the present results. We note that the experimental data for I_{NiNi} plotted by Maret *et al.* displays significantly more scatter than that for I_{NiAl} and I_{AlAl} and it is possible that this noise in the minority-minority partial structure factor could affect the shape of the peaks in the inverse-Fourier-transformed G_{NiNi}.

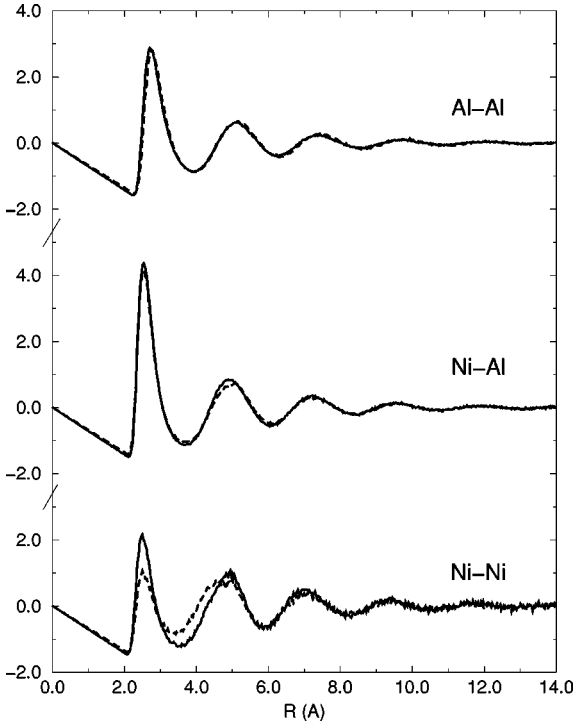

FIG. 2. Calculated reduced partial pair-correlation functions for liquid $Ni_{20}Al_{80}$ at $T=1300$ K. Solid and dashed lines are calculated results obtained with Voter-Chen and Foiles-Daw EAM potentials, respectively.

In Table I, we list EAM-calculated and measured[1] positions, R_{ij}, for each of the first peaks in G_{NiNi}, G_{AlAl}, and G_{NiAl}. The values of R_{ij} give an indication of the average first-neighbor *i-j* bond lengths in the liquid alloy. From the results in Table I, it can be seen that both EAM potentials predict that Ni-Al bonds are significantly shorter than the average $(R_{NiNi}+R_{AlAl})/2)$ of the Ni-Ni and Al-Al bond lengths. This result was also found in the calculations of Phuong *et al.*, as well as in the analysis of Maret *et al.*, and it is a further indication of the strong preference for heteroatomic nearest-neighbor bonds in Ni-Al alloys. With the exception of G_{NiNi}, as discussed above, the peak positions listed in Table I are found to be within 3% and 1% of the values obtained by Maret *et al.* and Phuong *et al.*, respectively.

As discussed in detail by Maret *et al.*, from the partial pair-correlation functions it is possible to compute values for the partial coordination numbers in the different coordination

TABLE I. Calculated nearest-neighbor distances (R), coordination numbers (z), and CSRO parameters (α) for liquid $Ni_{20}Al_{80}$ at $T=1300$ K. Experimental (Expt.) numbers are taken from Maret *et al.* (Ref. 1).

	R (VC)	R (FD)	R (Expt.)	z (VC)	z (FD)	z (Expt.)	α (VC)	α (FD)	α (Expt.)
Ni-Ni	2.52	2.50	2.36 2.98	1.87	1.78	1.65			
Ni-Al	2.54	2.52	2.54	10.27	10.12	10.91	−0.057	−0.064	−0.09
Al-Ni	2.54	2.52	2.54	2.57	2.53	2.71	−0.021	−0.033	
Al-Al	2.74	2.75	2.82	10.01	9.73	9.61			

shells around Ni and Al atoms. In Table I, VC and FD EAM results are listed for the first-neighbor partial coordination numbers z_{ij} in $Ni_{20}Al_{80}$ at $T=1300$ K, determined by integrating the partial pair-correlation functions out to a distance corresponding to the first minimum in the *total* pair-correlation function. We define z_{ij} as the average number of species j surrounding species i within the first coordination shell of the liquid. Also included in Table I are the values of z_{ij} taken from Maret *et al.*[1] We find that both EAM potentials underestimate slightly the total coordination number around each type of atom.

In terms of the z_{ij} it is possible to define CSRO parameters as follows:

$$\alpha_{ij}=1-\frac{z_{ij}}{c_j Z_i}, \tag{11}$$

where c_j is the concentration of species j and $Z_i=z_{ii}+z_{ij}$ is the total coordination number around species i. Negative values of α_{ij} indicate a preference for unlike-neighbor bonds. The EAM calculated values of α_{ij} are included in the last column of Table I, and they are found to be negative, indicating once again a preference for unlike-neighbor bonds. It is interesting to note that the degree of CSRO is enhanced around Ni atoms relative to the majority Al atoms. In particular, the values of α_{NiAl} obtained with both potentials are found to be roughly a factor of 2 larger than those for α_{AlNi}. The magnitudes of the calculated values for α_{NiAl} are found to be significantly lower than the value of -0.09 obtained from the measurements of Maret *et al.*[1] This result indicates that the degree of CSRO in a $Ni_{20}Al_{80}$ alloy at $T=1300$ K is apparently underestimated by both the VC and FD EAM potentials.

B. Thermodynamic properties

In Fig. 3 we show the results of EAM-MC calculations for atomic volumes (V) versus alloy composition at $T=1900$ K. Also included in Fig. 3 are results from experimental measurements[9] at $T=1923$ K. The measurements show that for concentrated alloys the atomic volumes are significantly smaller than would be expected from Vegard's law, i.e., a linear relationship between volume and concentration. The negative deviation from Vegard's law is again consistent with the presence of CSRO in the liquid. The EAM calculated results are in qualitative agreement with experiment, in that VC, FD, and LG results each reproduce the negative deviation from Vegard's law. However, there are significant quantitative discrepancies between the results obtained with the different potentials. In particular, the FD potentials overestimate (underestimate) the measured atomic volumes (densities) at all compositions. VC potentials give rise to improved agreement with experiment, although the deviation from Vegard's law for near-equiatomic alloys is underestimated. Overall, the best results are obtained with the LG potentials. The LG-EAM results provide a reasonable description of the atomic volume for alloys at all compositions, deviating by a few percent or less from experimental measurements. The results obtained in the present calculations are found to be qualitatively different from those obtained by Landa *et al.*[13] using both local and nonlocal pseudopotential-based thermodynamic pertubation theory. In the nonlocal calculations Landa *et al.* found nearly perfect agreement with experiment for pure-element atomic volumes, while results for alloys displayed an oscillating concentration dependence with regions of positive deviation from Vegard's law for Al-rich and Ni-rich compositions, and negative deviation near equiatomic concentrations. By contrast, the local-pseudopotential calculations gave rise to a concentration dependence for the volume which displayed practically no deviation from Vegard's law.

In Fig. 4 calculated and measured enthalpies of formation are plotted for liquid Ni-Al alloys. The calculated results were obtained at $T=1900$ K, while experimental measurements were performed at $T=1800$ K,[3] 1823 K,[2] and 1923 K.[5] In our calculations the temperature dependence of the enthalpies of formation was found to be very small. The different EAM potentials are all found to give very similar results over the entire range of composition. For Ni-rich alloys the calculated results are found to be in excellent agree-

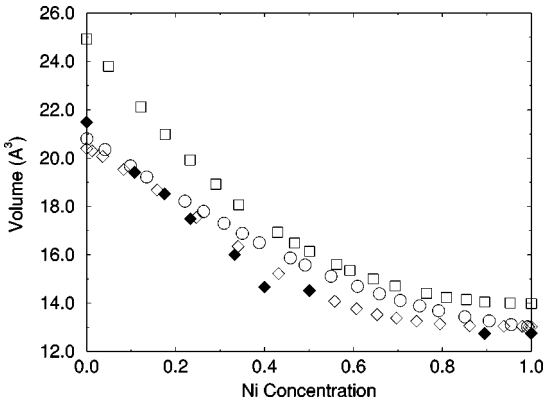

FIG. 3. Calculated and measured atomic volumes for liquid Ni-Al alloys. Open circle, square, and diamond symbols are calculated results obtained at $T=1900$ K with Voter-Chen, Foiles-Daw, and Ludwig-Gumbsch potentials, respectively. Filled symbols represent experimental data of Ayushina *et al.* (Ref. 9) at $T=1923$ K.

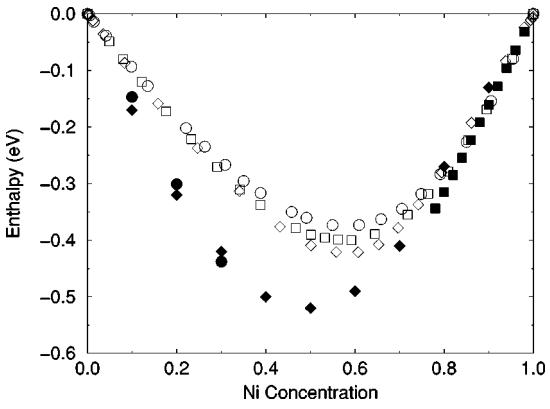

FIG. 4. Calculated and measured enthalpies of formation for liquid Ni-Al alloys. Open circle, square, and diamond symbols are calculated results obtained at $T=1900$ K with Voter-Chen, Foiles-Daw, and Ludwig-Gumbsch potentials, respectively. Filled circle, square, and diamond symbols represent experimental data at $T=1800$ K [Sudovtseva *et al.* (Ref. 3)], $T=1823$ K [Grigorovitch and Krylov (Ref. 2)] and 1900 K [Sandakov *et al.* (Ref. 5)], respectively.

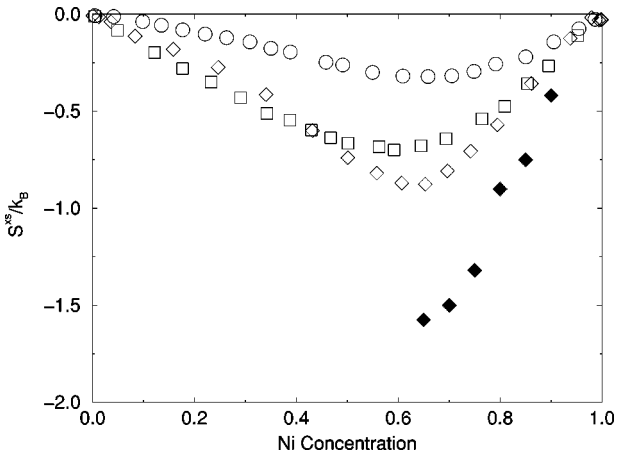

FIG. 5. Calculated and measured entropies of mixing. Open circle, square, and diamond symbols are calculated results obtained at $T=1900$ K with Voter-Chen, Foiles-Daw, and Ludwig-Gumbsch potentials, respectively. Filled diamond symbols correspond to measured values at $T=1923$ K from Batalin *et al.* (Ref. 10). The dashed line represents the ideal entropy of mixing.

ment with experimental measurements. However, as the concentration of Al is increased beyond roughly 25 at. % the magnitudes of the calculated enthalpies of formation are consistently underestimated compared to measurements. The largest discrepancy is found near the composition of 40 at. % Ni where calculated and measured enthalpies of formation differ by roughly 0.15 eV/atom. The fact that the calculated enthalpies of mixing are smaller in magnitude than the measured values for Al-rich alloys is consistent with the finding that the EAM potentials also underestimate the degree of CSRO, as discussed above. The overall level of agreement between the experimental and EAM-calculated results shown in Fig. 4 is significantly better than that obtained by Landa *et al.*[13] who found discrepancies as large as 0.5 and 1.5 eV/atom in the local and nonlocal pseudopotential calculations, respectively.

Calculated ($T=1900$ K) and measured ($T=1923$ K) (Ref. 10) entropies of mixing are plotted in Fig. 5 as excess quantities ($S^{xs}=\Delta S-\Delta S_{\text{ideal}}$ is the difference between the total entropy of mixing $[\Delta S]$ and the ideal entropy of mixing $[\Delta S_{\text{ideal}}]$). All calculated and measured values of S^{xs} shown in Fig. 5 are negative. However, there are large differences found in the magnitudes of the calculated and measured values. The best overall agreement between calculated and experimental values of S^{xs} is obtained with the LG EAM potentials for alloys with greater than 80% Ni. The discrepancy between LG results and experiment for the more Al-rich compositions might be due to the underestimation of the degree of CSRO by the EAM for these alloys, as well as the neglect of electronic contributions in our calculations of thermodynamic properties of mixing. The level of agreement between LG-EAM calculations and experiment is comparable to that obtained in the calculations by Landa *et al.*[13] using the nonlocal pseudopotential formalism (local pseudopotential results produced only very small values for the excess entropy).

The differences between the FD, VC, and LG calculated entropies of mixing shown in Fig. 5 can be understood based upon the results for atomic volumes plotted in Fig. 3. Specifically, an important contribution to the entropy of mixing in a liquid alloy is the so-called hard-sphere entropy (S_{HS}) (see, for example, Ref. 61–63). S_{HS} is expressed in terms of the packing fraction and its contribution to the entropy of mixing reflects the concentration dependence of the ''excess volume.'' If we assume a simple model where the hard-sphere radii for each constituent element in the alloy is independent of concentration, ΔS_{HS} can be written in terms of the deviation from Vegard's law. We have used the hard-sphere radii for Ni-Al derived by Saadeddine *et al.*[15] and the atomic volume results plotted in Fig. 3 to compute ΔS_{HS} for Ni-Al as predicted by the three different EAM potentials. It is found that ΔS_{HS} is large and negative and that the differences in the calculated values of ΔS shown in Fig. 5 correspond well with the differences in ΔS_{HS} predicted by the three EAM potentials. In particular, for an equiatomic NiAl liquid alloy, the differences between the FD, VC, and LG values for ΔS_{HS} are $\Delta S_{\text{HS}}(\text{FD})-\Delta S_{\text{HS}}(\text{VC})=-0.35$ and $\Delta S_{\text{HS}}(\text{FD})-\Delta S_{\text{HS}}(\text{LG})=0.16$ at $T=1900$ K. The differences in these three numbers correspond very well with the values of $\Delta S(\text{FD})-\Delta S(\text{VC})$ and $\Delta S(\text{FD})-\Delta S(\text{LG})$ obtained from Fig. 5.

In Fig. 6 calculated and measured values of the Ni and Al activities in liquid Ni-Al alloys are plotted. Measurements were performed at $T=1873$ K (Ref. 6) and 2000 K (Ref. 7) and calculated results are plotted at $T=1900$ K. Both experiment and calculations predict activities which deviate strongly from the ideal values (i.e., activities equal to concentration). The large negative deviations from ideal values displayed by the activities are again consistent with a strongly ordering mixture. It is interesting to note that the level of agreement between calculations and measurements obtained for activities is better overall than that obtained for either the enthalpies (Fig. 4) or entropies (Fig. 5) of mixing. The very good agreement between experiment and calculations displayed in Fig. 6 therefore largely reflects a cancellation of the errors associated with the enthalpy and entropy contributions to the free energy of mixing.

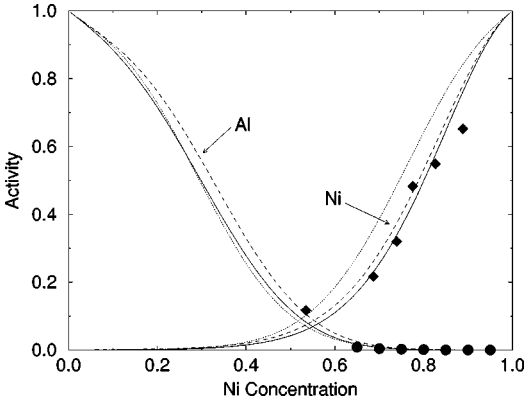

FIG. 6. Calculated and measured activities for liquid Ni-Al alloys. Dashed, solid, and dash-dotted lines give Voter-Chen, Foiles-Daw, and Ludwig-Gumbsch calculated results at $T=1900$ K, respectively. Filled circles correspond to measured values for Al from Vachet *et al.* (Ref. 6) at $T=1873$ K. Filled diamonds represent measured values for Ni from Johnson and Palmer (Ref. 7) at $T=2000$ K.

C. Atomic-transport properties

The viscosity as determined from the MD simulations at 1900 K is shown in Fig. 7 as a function of Ni concentration. The FD potentials yield a viscosity which is consistently lower than the VC potential and the LG potential exhibits a trend with composition similar to the other two potentials but is displaced upward from the VC values by approximately 0.8 cP. The behavior of the viscosity with the choice of potential can perhaps be rationalized with reference to the equilibrium volume plot of Fig. 4. The FD result yields the lowest density and also predicts the lowest viscosity whereas the LG potential predicts the highest density and viscosity. The well known Enskog theory[64] of transport properties in fluids is consistent with the density-viscosity behavior shown in Figs. 4 and 7. There appear to be, however, other factors which are important in the viscosity of NiAl alloys. All three potentials exhibit an increasing viscosity with increasing Ni content but with small maxima superimposed in the vicinity of the compositions Ni_3Al and NiAl. The

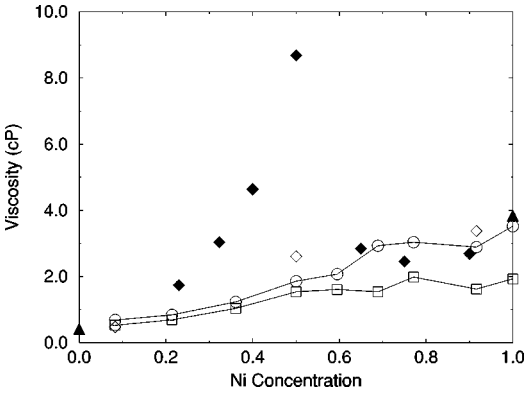

FIG. 7. Calculated and measured viscosities for liquid Ni-Al alloys at 1900 K. Open circles, squares, and diamonds correspond to the Voter-Chen, Foiles-Daw and Ludwig-Gumbsch potentials, respectively. Filled diamonds are the measured viscosities for alloys taken from Petrushevskii *et al.* (Ref. 11) and filled triangles represent results for elements at $T=1900$ K taken from (Ref. 65).

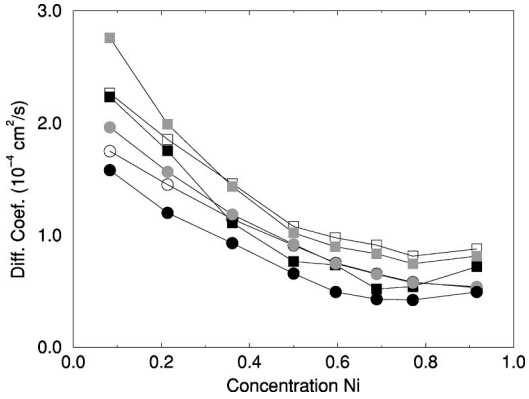

FIG. 8. Computed diffusion coefficients for Ni-Al liquid alloys at 1900 K. The circles represent results from the Voter-Chen potential and the squares refer to Foiles-Daw results. The open symbols denote D_{Ni}, the gray symbols are D_{Al}, and the filled symbols refer to the mutual diffusivity D_{NiAl}.

maxima which are not associated with any features in the density curves, most likely arise due to an increased ordering tendency at these concentrations.

It is of interest to compare the MD viscosity results with the experimental measurements[11,65] plotted as filled symbols in Fig. 7. For Ni-rich compositions the LG and VC simulations agree quite well with experiment, the FD computations slightly underestimate the measured values. However, at the equiatomic composition there is a very sharp peak in the measured viscosity (approximately 9 cP) which is not reproduced by any of the EAM potentials for Ni-Al. Landa *et al.*[13] investigated the viscosity of Ni-Al liquids within the framework of the Enskog model using both local and nonlocal pseudopotential formalisms, where in the latter approach a resonant contribution was incorporated in order to take into account explicitly charge transfer. The local pseudopotential theory gave a viscosity similar to the calculated results shown in Fig. 7, i.e., it was also unable to reproduce the large experimental peak at the NiAl concentration. On the other hand, the nonlocal resonant pseudopotential result did show a maximum near the 50% composition but the viscosity was overestimated by roughly a factor of 2. Further theoretical work is required to understand more completely the origins of the discrepancies between the different calculated and experimental results presented in Fig. 7 and Ref. 13.

Figure 8 shows the three diffusion coefficients, D_{Ni}, D_{Al}, and D_{NiAl}, as a function of concentration for the VC and FD potentials. The diffusivities predicted by FD are consistently greater than the VC calculations. The qualitative trend in Fig. 8 is very similar to the equilibrium volume plot of Fig. 4, again illustrating the importance of density on the transport properties. It should also be noted that the calculated values of D_{Ni} are very nearly equal to those for D_{Al} except at the Al-rich concentrations.

For each potential the mutual diffusion coefficient is found to lie below the values of D_{Ni} and D_{Al} over the entire composition range. This result can be explained with reference to the work of Jacucci and McDonald[66] and Hansen and McDonald.[67] These authors point out that if velocity cross correlations given by $\langle \vec{u}_i(t)\cdot\vec{u}_j(0)\rangle$ $i\neq j$ are negligible then the mutual diffusion coefficient is just the weighted average of the two individual diffusivities, i.e., $D_{\mathrm{NiAl}}=c_{\mathrm{Al}}D_{\mathrm{Ni}}$

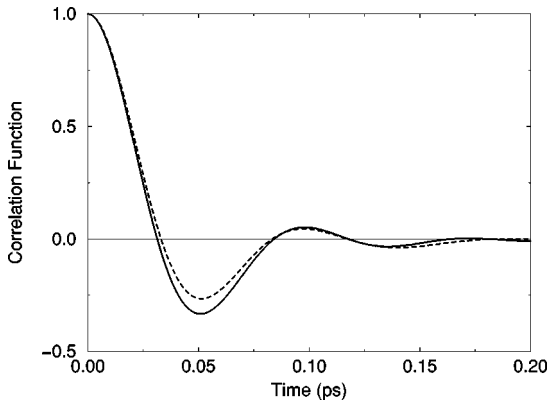

FIG. 9. Interdiffusion flux correlation function for a Ni concentration of 0.771 at 1900 K. The solid line refers to the correlation function defined in Eqs. (6) and (7) whereas the dashed lined is formed from the weighted sum of the individual velocity-velocity correlation functions for Ni and Al.

$+c_{\mathrm{Ni}}D_{\mathrm{Al}}$. Such a relationship holds for the case of mixtures of Lennard-Jones liquids,[66] but does not hold for diffusion in strongly ordering systems such as the molten salts studied by Hansen and McDonald[67] where the interionic potential included a Coulombic contribution as well as an inverse-power repulsion. The Ni-Al system studied here is another example of an ordering system and thus one would expect similar qualitative results as obtained in the aforementioned molten salt investigation. Figure 9 shows two velocity correlation functions at 1900 K and for a Ni concentration of 0.771. Both functions have been normalized by their values at $t=0$. The bottom curve refers to the correlation function generated by the interdiffusion flux defined in Eqs. (6) and (7) whereas the top curve corresponds to the weighted sum of the two individual velocity-velocity correlation functions for Ni and Al. The results of Fig. 9 are in fact very similar to the Hansen and McDonald result (their Fig. 4) and illustrate that ordering type potentials will yield a lower mutual diffusivity than that predicted by the simple weighted average argument. Physically, the lowering of the mutual diffusion coefficient stems from the fact that motion of a pair of strongly bonded Ni-Al atoms contributes to the self diffusion but does not contribute to the mutual diffusion.[58]

IV. SUMMARY

Structural, thermodynamic, and atomic-transport properties of liquid Ni-Al alloys have been studied using a combination of classical MC and MD simulations based upon three different EAM potentials. Calculated liquid structure factors and pair-correlation functions obtained with each potential are found to be very similar and for a $Ni_{20}Al_{80}$ alloy at $T=1300$ K the main features of the measured partial structure factors[1] are well reproduced. The relative insensitivity of simulated liquid structures to the differences in the EAM potentials considered in this study is perhaps not surprising since the main features of the liquid alloy structure appear to be controlled by two factors which are reasonably well described by each potential: the relative sizes of Ni and Al, and the strong preference for the formation of unlike-atom (Ni-Al) bonds.

At $T=1900$ K atomic denisties and thermodynamic properties of mixing calculated by all three EAM potentials featured composition dependences in qualitative agreement with experimental measurements. In particular, each potential predicts atomic volumes which display a large negative deviation from Vegard's law, large and negative enthalpies of mixing, and strong deviation from ideal-solution behavior for entropies of mixing and activities. The levels of quantitative agreement between experiment and theory obtained with the three EAM potentials were significantly different. In particular, the FD potentials overestimate the atomic volume at all concentrations, while both VC and LG potentials give rise to atomic densities in good agreement with experimental measurements. The differences in the atomic volumes predicted by the three EAM potentials are found to be reflected in the values of the viscosities and entropies of mixing computed by MD and MC, respectively. The largest discrepancies beteween calculated and measured thermodynamic and atomic-transport properties were found for Al-rich alloys where the magnitudes of the enthalpies and entropies of mixing and viscosities are significantly underestimated. Overall, the best level of agreement between experiment and theory was obtained with the LG potentials, demonstrating that the VC-form for the pair potentials and the extra alloy information included in the fitting of the potentials by Ludwig and Gumbsch lead to an improved description of the properties of liquid Ni-Al alloys.

The EAM potentials, and the VC and LG potentials, in particular, are found to provide a very realistic description of a wide variety of structural, thermodynamic, and atomic-transport properties for Ni-rich liquid alloys, even though no liquid data was included in the fitting of the potentials. Significant discrepancies between experimental measurements and calculations for alloys with near-equiatomic and Al-rich compositions are found with all three potentials, suggesting that these shortcomings may reflect inaccuracies associated with the EAM description of cohesion for transition-metal-Al alloys. Therefore, further calculations of liquid alloy properties based upon interatomic potentials derived from tight-binding theory[14] or pseudopotentials[68] would be of interest.

ACKNOWLEDGMENTS

This work was supported by the Office of Basic Energy Science, Division of Materials Science, of the U. S. Department of Energy under Contract NO. DE-AC04-94AL85000. We thank M. I. Baskes for a critical reading of the manuscript.

*Present address: Dept. of Materials Science and Engineering, Massachusetts Institute of Technology, Cambridge, MA 02139-4302.

[1] M. Maret, T. Pomme, A. Pasturel, and P. Chieux, Phys. Rev. B **42**, 1598 (1990).
[2] K.V. Grigorovitch and A.S. Krylov, Thermochim. Acta **314**, 255 (1998).
[3] V.S. Sudovtseva, A.V. Shuvalov, N.O. Sharchina, Rasplavy No. **4**, 97 (1990).
[4] U.K. Stolz, I. Arpshofen, F. Sommer, and B. Predel, J. Phase Equilib. **14**, 473 (1993).
[5] V.M. Sandakov, Yo O. Esin, and P.V. Geld, Russ. J. Phys. Chem. **45**, 1798 (1971).
[6] F. Vachet, P. Desre, and E. Bonnier, C. R. Acad. Sci. URSS **260**, 453 (1965).
[7] G.R. Johnson and L.D. Palmer, High Temp.-High Press. **12**, 261 (1980).
[8] K. Hilpert, M. Miller, H. Gerads, and H. Nickel, Ber. Bunsenges. Phys. Chem. **94**, 40 (1990).
[9] G.D. Ayushina, E.S. Levin, and P.V. Geld, Russ. J. Phys. Chem. **43**, 2756 (1969).
[10] G. I. Batalin, E. A. Beloborodova, and V. G. Kazimirov, *Thermodynamics and the Constitution of Liquid Al Based Alloys* (Metallurgy, Moscow, 1983).
[11] M.S. Petrushevskii, E.C. Levin, and P.V. Geld, Russ. J. Phys. Chem. **45**, 1719 (1971).
[12] C. Colinet, A. Bessoud, and A. Pasturel, J. Phys.: Condens. Matter **1**, 5837 (1989).
[13] A.I. Landa, A.A. Yuryev, A.V. Ruban, E.G. Gurskaya, Yu K. Kovneristyi, and N.A. Vatolin, J. Phys.: Condens. Matter **3**, 9229 (1991); Yu.K. Kovneristyi, N.A. Vatolin, E.G. Gurskaya, A.I. Landa, M.V. Romankevitch, and A.A. Yuryev, J. Non-Cryst. Solids **117/118**, 589 (1990).
[14] L.D. Phuong, D.N. Manh, and A. Pasturel, Phys. Rev. Lett. **71**, 372 (1993); Mol. Simul. **20**, 79 (1997).
[15] S. Saadeddine, J.F. Wax, B. Grosdidier, J.G. Gasser, C. Regnaut, and J.M. Dubois, Phys. Chem. Liq. **28**, 221 (1994).
[16] A. Pasturel, C. Colinet, A.T. Paxton, and M. van Schilfgaarde, J. Phys.: Condens. Matter **4**, 945 (1992).
[17] M.S. Daw and M.I. Baskes, Phys. Rev. B **29**, 6443 (1984).
[18] M.S. Daw, S.M. Foiles, and M.I. Baskes, Mater. Sci. Rep. **9**, 251 (1993); S. M. Foiles, in *Equilibrium Structure and Properties of Surfaces and Interfaces*, edited by A. Gonis and G. M. Stocks, Vol. 300 of NATO Advanced Study Institute, Seris B: Physics (Plenum, New York, 1992).
[19] S.M. Foiles, Phys. Rev. B **32**, 3409 (1985).
[20] Y. Waseda, *The Structure of Non-Crystalline Materials* (McGraw-Hill, New York, 1980).
[21] S.M. Foiles and J.B. Adams, Phys. Rev. B **40**, 5909 (1989).
[22] J.B. Adams and S.M. Foiles, Phys. Rev. B **41**, 3316 (1990).
[23] J.M. Holender, J. Phys.: Condens. Matter **2**, 1291 (1990).
[24] J.M. Holender, Phys. Rev. B **41**, 8054 (1990).
[25] L.M. Holzman, J.B. Adams, S.M. Foiles, and W.N.G. Hitchon, J. Mater. Res. **6**, 298 (1991).
[26] R. LeSar, R. Najafabadi, and D.J. Srolovitz, J. Chem. Phys. **94**, 5090 (1991).
[27] G.M. Bhuiyan, M. Silbert, and M.J. Stott, Phys. Rev. B **53**, 636 (1996).
[28] T.M. Brown and J.B. Adams, J. Non-Cryst. Solids **180**, 275 (1995).
[29] B. Sadigh and G. Grimvall, Phys. Rev. B **54**, 15 742 (1996).
[30] A. Posada-Amarillas and I.L. Garzon, Phys. Rev. B **53**, 8363 (1996).
[31] J.I. Akhter and K. Yaldram, Int. J. Mod. Phys. C **8**, 1217 (1997).
[32] L.H. Wang, H.Z. Liu, K.Y. Chen, and Z.Q. Hu, Physica B **239**, 267 (1997).
[33] J. Lu and J.A. Szpunar, Philos. Mag. A **75**, 1057 (1997).
[34] J. Cai and Y.Y. Ye, Acta Phys. Sin. **5**, 431 (1996).
[35] K.Y. Chen, H.B. Liu, X.P. Li, Q.Y. Han, and Z.Q. Hu, J. Phys.: Condens. Matter **7**, 2379 (1995).
[36] J.R. Morris, C.Z. Wang, K.M. Ho, and C.T. Chan, Phys. Rev. B **49**, 3109 (1994).
[37] J.R. Ray and R.J. Wolf, J. Chem. Phys. **98**, 2263 (1993).
[38] J. Mei and J.W. Davenport, Phys. Rev. B **46**, 21 (1992).
[39] R.N. Barnett and U. Landman, Phys. Rev. B **44**, 3226 (1991).
[40] J. Mei, J.W. Davenport, and G.W. Fernando, Phys. Rev. B **43**, 4653 (1991).
[41] M.M.G. Alemany, C. Rey, and L.J. Gallego, Phys. Rev. B **58**, 685 (1998).
[42] Q. Xie and M.C. Huang, Phys. Status Solidi B **186**, 383 (1994).
[43] O.R. de la Fuente and J.M. Soler, Phys. Rev. Lett. **81**, 3159 (1998).
[44] F.J. Cherne III and P.A. Deymier, Scr. Mater. **39**, 1613 (1998).
[45] P. Ballone and S. Rubini, Phys. Rev. B **51**, 14 962 (1995); Surf. Sci. **342**, L1116 (1995); Phys. Rev. Lett. **77**, 3169 (1996).
[46] K.Y. Chen, X.W. Sha, X.M. Zhang, and Y.Y. Li, Mater. Sci. Eng., A **214**, 139 (1996).
[47] M. Shimono and H. Onodera, Mater. Trans., JIM **39**, 147 (1998).
[48] T. Aihara, K. Aoki, and T. Masumoto, Mater. Sci. Eng., A **179**, 256 (1994).
[49] M.H. Sabochick and N.Q. Lam, Phys. Rev. B **43**, 5243 (1991).
[50] H.B. Liu, K.Y. Chen, and Z.Q. Hu, J. Mater. Sci. Technol. **13**, 117 (1997).
[51] M.I. Baskes, Acta Metall. Sin. **8**, 287 (1995).
[52] A.F. Voter and S.P. Chen, in *Characterization of Defects in Materials*, edited by R. W. Siegel *et al.*, MRS Symposia Proceedings No. 82 (Materials Research Society, Pittsburgh, 1978), p. 175.
[53] S.M. Foiles and M.S. Daw, J. Mater. Res. **2**, 5 (1987).
[54] M. Ludwig and P. Gumbsch, Modell. Simul. Mater. Sci. Eng. **3**, 533 (1995).
[55] M.P. Allen and D.J. Tildesley, *Computer Simulation of Liquids* (Clarendon, Oxford, 1987).
[56] S.M. Foiles, M.I. Baskes, and M.S. Daw, Phys. Rev. B **33**, 7983 (1986).
[57] A.T. Paxton, in *Proceedings of TMS Symposium Twinning in Advanced Materials* (TMS, Pittsburgh, 1993).
[58] J.P. Hansen and I.R. McDonald, *Theory of Simple Liquids* (Academic, London, 1976)
[59] T.E. Faber and J.M. Ziman, Philos. Mag. **11**, 153 (1965).
[60] A.B. Bhatia and D.E. Thornton, Phys. Rev. B **2**, 3004 (1970).
[61] N.W. Ashcroft and D. Stroud, in *Solid State Physics: Advances in Research and Applications*, edited by H. Ehrenreich, F. Seitz, and D. Turnbull (Academic, New York, 1978), Vol. 33, p.1.
[62] A. Pasturel, J. Hafner, and P. Hicter, Phys. Rev. B **32**, 5009 (1985).

[63] J. Hafner, A. Pasturel, and P. Hicter, Z. Metallkd. **76**, 432 (1985).
[64] S. Chapman and T. G. Cowling, *The Mathematical Theory of Non-Uniform Gases* (Cambridge University Press, London, 1970).
[65] *Smithells Metal Reference Book*, edited by E. A. Brandes and G. B. Brook (Butterworth-Heinemann, Oxford, 1998).
[66] G. Jacucci and I.R. McDonald, Physica A **80A**, 607 (1975).
[67] J.P. Hansen and I.R. McDonald, Phys. Rev. A **11**, 2111 (1975).
[68] J.A. Moriarty and M. Widom, Phys. Rev. B **56**, 7905 (1997); M. Widom and J.A. Moriarty, *ibid.* **58**, 8967 (1998).